

Indirect Force measurement of Micromilling with an Active Magnetic Bearing spindle

R.S. Blom^{1,2*}, A.M. Hoogstrate¹, P.M.J. Van den Hof², H.H. Langen¹

¹ Precision and Microsystems Engineering

² Delft Center for Systems and Control

Delft University of Technology, Mekelweg 2, 2628 CD Delft, The Netherlands

* corresponding author: r.s.blom@tudelft.nl

Abstract

While scaling down the toolsize in micromilling, the challenge of maintaining a stable and accurate machining process increases. Hence robust online process monitoring and control are important for obtaining a reliable micromilling process. Online indirect cutting force measurement is proposed that uses the active nature of an Active Magnetic Bearing spindle. Using a model-based estimation scheme, force measurements are obtained using data from the displacement sensors and coil current sensors in the magnetic bearing system. It is demonstrated that the bandwidth that can be achieved with this approach suffices for the micromilling application.

1 INTRODUCTION

The main motivation for scaling conventional milling to the microdomain is that it enables the fabrication of individual micro-components with 3D features. Applications of such components can be found in areas like Medical, Aerospace, Automotive, and Electronics & Communications. Reducing the tool diameter to the range below 1 mm results in a number of issues that make micro milling fundamentally different from conventional machining. This is due to a change of dominant effects when scaling, which include vibrations, the influence of tool geometry, offsets and rigidity, temperature effects and workpiece homogeneity. As a result process stability, surface generation and process accuracy are affected. To obtain a stable, reliable and high quality micromilling process, much research is still needed. This addressed from different angles:

- Efforts are done to increase more understanding about the chip formation at the micro scale, which is to be used for process optimization and tool design;
- Research is done to develop new concepts for meso-scale machine design to realize faster and more precise machinery;
- Investigated are methodologies enabling process monitoring and control during 3D micromilling. The presented research is included in this theme.

Implementation of monitoring and control techniques tailored to the challenges of this process is of paramount importance. To reach the desired accuracies, more control mechanisms are

needed alongside highly accurate motion control of the tooltip. This may include vibration control, cutting force control, tool deflection control and (thermal) error compensation. Furthermore, workpiece quality will benefit from tool condition monitoring techniques. In the micro scale, wear of the tool edge has a significant impact on the process quality and stability. Tool wear monitoring may allow for better control of the surface roughness, burr formation, and other process phenomena. Tool breakage avoidance and detection is needed to prevent damage to workpiece and machine.

In all of the above mentioned techniques two elements are essential: (1) obtaining reliable information about the process and (2) using this information online in a closed-loop setting to adapt the milling process. In this research our objective is to perform both steps in a model-



Figure 1: Experimental setup.

based setting, while including measures to guarantee performance under disturbances and model uncertainty.

Indirect force measurement

In conventional cutting, signals that are typically used to obtain realtime information about the cutting process are measurements of the cutting forces and the spindle power. Due to small powers and the high required bandwidths involved in micromilling, we consider the first.

Obviously, direct measurement of the cutting forces using a dynamometer setup could be pursued. However, like in conventional cutting, disadvantages of direct force measurement in micromilling include the equipment's high cost, fragility to overload, influence on machine dynamics and the practical issues of including it in the machining space. In conventional cutting these disadvantages have led researchers to investigate indirect force signal estimation by using information from elsewhere in the machine. This includes information from sensors (such as displacements sensors) or information from active components of the machine. In this research we propose indirect force measurement using the Active Magnetic Bearings (AMB) of the milling spindle.

For a micromilling application active magnetic bearings combine a number of favorable features. First, the maximum achievable surface speed of magnetic bearings is much larger than rolling element bearings. Rotational speeds up to the limit of material strength are possible. There is virtually no wear and no need for lubrication. Second, because they are non-contacting, magnetic bearings are not prone to the same thermal problems as conventional bearings at high speeds. Last, the active nature opens a range of monitoring and control possibilities, a feature that is unique for magnetic bearings. Citing Bleuler [1]: *[...] this type of bearing has a great potential for increased safety, reliability, and on-line machining process control [...]. Instantaneous and precise signals for shaft position, bearing current, and thus bearing force are automatically and constantly available. They permit permanent monitoring of lead forces, moments and vibrations. These signals can be exploited for sophisticated machining control for various purposes including machining quality, safety, maintenance, etc..*

Some results have been published. Müller [2] explored the application of an AMB spindle for cutting force estimation, tool breakage detection and tool wear monitoring. The techniques applied by Müller are basic, but demonstrate

the concept of utilizing AMB spindle for online process monitoring and control purposes. Auchet [3] uses the AMB spindle for indirect force estimation, where the transfer functions linking the unknown cutting force with the command voltages are determined experimentally at zero rpm. Still, the results are in good agreement with force measurements from a dynamometer platform for low frequencies.

Our approach to indirect force measurement is model-based estimation that uses data which is already available from the magnetic bearings. In this paper we will present simulation results which are based on the micromilling setup that has been realized in our laboratory. This has been organized as follows. First in section 2 we will briefly discuss AMB technology, followed by a description of the experimental setup in section 3. In section 4 the modeling of this setup is discussed, which is used in section 5 to construct a model-based cutting force estimator. Simulation results of the force estimator are included in section 6.

2 MAGNETIC BEARING TECHNOLOGY

Unlike conventional bearings systems, the rotor of an AMB spindle is carried by a magnetic field. The most common configuration for this is depicted in figure 2. At the front side of the rotor two magnetic actuators control the position in the x and y plane; similarly two actuators control the x and y position of the rotor at rear side. An axial bearing is added to control the position of the rotor in the z-direction. A motor rotates the spindle in the single left uncontrolled DOF. One actuator consists of two coils at opposite sides of the rotor, which are most commonly configured in *differential drive mode*. In this configuration both coils create a bias flux of the same size. However, a control current that is fed to the coils and that makes adjustments to this bias flux has opposite sign. This implies that a nonzero control current will increase the flux in one coil by the same amount it is reduced in the other, resulting in a net force on the rotor. This effect is used to control the position of the rotor. To do this, the current position of the rotor is measured by a displacement sensor and taken as input by a controller to command the current levels in the coils using a current amplifier.

3 EXPERIMENTAL SETUP

A picture of the experimental setup is found in figure 1. A three axis milling machine is created using a horizontal XY stage to position the workpiece and a vertically mounted Z-stage for

translation of the spindle. Together these stages are mounted on a granite table with a bridge for the Z-axis. All stages are manufactured by Aerotech. The horizontal drives have linear motors, with positioning accuracy of $<0.3 \mu\text{m}$ and a repeatability of $<0.12 \mu\text{m}$. The vertical drive has a lead screw and has a positioning accuracy of $0.75 \mu\text{m}$ and a repeatability of $0.1 \mu\text{m}$.

The selected AMB spindle is from EAAT GmbH Chemnitz (Elektrische Automatisierungs- und Antriebstechnik). This is a spindle with a maximum rotational speed of 120.000 rpm, which is relatively high for currently available AMB spindles. The rotor length is 250 mm. The controller of the bearings is an analog PID of which the exact parameters are unknown. The resolution of the displacement sensors of the AMBs is $0.1 \mu\text{m}$. The AMB controller hardware also provides measurements of the currents through the coils with an accuracy of 1mA.

4 MODELING

4.1 Requirements

The cutting force is estimated from measurements of the currents and displacements in a model-based setting. Important aspects of this approach are:

- **Model:** a model is required of the transfer function from cuttings force acting on the tooltip to the displacement of the spindle shaft at the location of the displacement sensors in the bearings. Here the gyroscopic effects due to the high rotational speeds need to be included. Furthermore, a

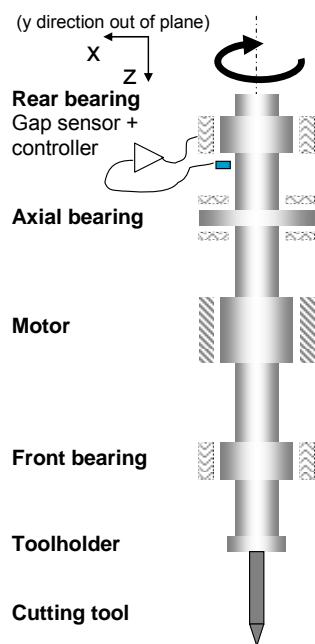


Figure 2: Schematic of Active Magnetic Bearing spindle.

model is needed to predict the force from the magnetic bearings on the spindle. To develop an estimator also an appropriate model for the cutting forces is needed.

- **Bandwidth:** The bandwidth requirement on any force measurement approach in micromilling is high due to high rotational speeds. Rotational speeds of 120,000 rpm will lead to cutting force signals with base frequency of 2 kHz. The question that we will answer is what will be the maximum achievable bandwidth with the presented approach.
- **Disturbance modeling:** apart from measurement inaccuracy of the displacement sensors in the bearings, other disturbances need to be accounted for. These are related to the mass imbalance and to geometric errors of the spindle system. As a result, even when rotating free of external forces we will obtain a non-zero response of our system. These readings will be dependent on the rotational frequency.

In this paper we concentrate on the first two aspects. Disturbance modeling will be addressed when dealing with real as opposed to simulated data.

In the following subsections we will describe the model of the spindle and the magnetic bearings. This model is used in section 5 to derive a force estimator. In this research, we limit attention to estimation of the cutting forces in x and y direction. Particularly when milling with square end mills the cutting forces in x and y direction are of most interest.

4.2 Model of a rotating spindle

The spindle, including toolholder and tool, is modeled as a series of rigidly connected flexible beam elements. Each of these beam elements is modeled as a flexible body with constant circular cross-section and certain length (see figure 3a). This element has two nodes, with four degrees of freedom each (displacement in x and y direction and rotations along these axes, denoted by θ and ψ respectively). Hence we obtain the following vector of generalized coordinates:

$$\xi = [x_1 \quad y_1 \quad \theta_1 \quad \psi_1 \quad x_2 \quad y_2 \quad \theta_2 \quad \psi_2]^T$$

The beam is assumed to rotate around its z-axis with constant rotational speed Ω . By calculating the kinetic and potential energies along the beam element as function of the generalized coordinates, while assuming values for the mass density, Young's modulus and Poisson

ratio of the material, by applying Lagrange's theorem we find the following equation of motion for the beam element:

$$\mathbf{M}\ddot{\xi} + \mathbf{G}\dot{\xi} + \mathbf{K}\xi = \mathbf{F}_{ext} \quad (1)$$

with \mathbf{M} the mass matrix, \mathbf{G} the gyroscopic matrix and \mathbf{K} the stiffness matrix of our system. \mathbf{M} and \mathbf{K} are symmetric; \mathbf{G} is skew-symmetric and depending on Ω . \mathbf{F}_{ext} is the vector of external forces and moments acting on the beam.

An FE model of the spindle is obtained by modeling it as a finite series of rigidly connected beam elements. Consider beam element A of which its right node is rigidly connect to the left node of beam element B. Let $\xi_i = [x_i \ y_i \ \theta_i \ \psi_i]^T$, with $i=1,2$ denote the generalized coordinates of the left and right node of a beam respectively. Rigid connection of beam element A and B can be expressed mathematically as $\xi_2^A = \xi_1^B$. To derive the equation of motion of the connected system, define the extended coordinate vector \mathbf{x} :

$$\mathbf{x} = [\xi_1^A \ \xi_2^A \ \xi_2^B]^T = [\xi_1^A \ \xi_1^B \ \xi_2^B]^T$$

If we write the mass matrices of beam A and B as

$$\mathbf{M}^A = \begin{bmatrix} \mathbf{M}_{11}^A & \mathbf{M}_{12}^A \\ \mathbf{M}_{21}^A & \mathbf{M}_{22}^A \end{bmatrix}, \quad \mathbf{M}^B = \begin{bmatrix} \mathbf{M}_{11}^B & \mathbf{M}_{12}^B \\ \mathbf{M}_{21}^B & \mathbf{M}_{22}^B \end{bmatrix}$$

and decompose the \mathbf{G} and \mathbf{K} matrices accordingly, then it can easily be verified that the connected system can be described as

$$\mathbf{M}\ddot{\mathbf{x}} + \mathbf{G}\dot{\mathbf{x}} + \mathbf{K}\mathbf{x} = \mathbf{F}_{ext} \quad (2)$$

with

$$\mathbf{M} = \begin{bmatrix} \mathbf{M}_{11}^A & \mathbf{M}_{12}^A & 0 \\ \mathbf{M}_{21}^A & \mathbf{M}_{22}^A + \mathbf{M}_{11}^B & \mathbf{M}_{11}^B \\ 0 & \mathbf{M}_{21}^B & \mathbf{M}_{22}^B \end{bmatrix}$$

and \mathbf{G} and \mathbf{K} having a similar structure. An FE model of the rotor can be obtained by repeating the above procedure. The number of elements needed is determined by the diameter variations of the rotor, as well as the number of structural modes of interest.

As is clear from the above analysis, this model does not include material damping. For material damping no straightforward modeling approach is available from first principles. Here we have applied the principle of Rayleigh damping, which implies that a damping matrix \mathbf{D} is added to \mathbf{G} . This matrix is a linear combination of the mass and stiffness matrix:

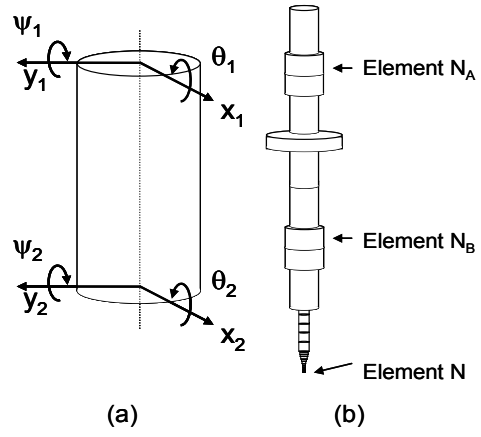


Figure 3: FE model of the spindle.

$$\mathbf{D} = \alpha \mathbf{M} + \beta \mathbf{K} \quad (3)$$

This introduces two degrees of freedom, which can be chosen such that the damping of the first two eigenmodes are as desired.

Neither present in this model is the negative stiffness of the motor. Although not included, this can quite easily be accounted for in this model by adding an extra stiffness matrix. Experimental validation of the model will demonstrate the necessity of this.

Lastly, not included also are misalignments between spindle and tool. These will be accounted for in a later stage when modeling the disturbances.

4.3 Model of the magnetic bearings

It is well established that the force that is exerted by a magnetic bearing in differential driving mode can be modeled by the following nonlinear equation [4]

$$F = \lambda \left[\left(\frac{i_{bias} + i}{g_0 - x} \right)^2 - \left(\frac{i_{bias} - i}{g_0 + x} \right)^2 \right] \quad (4)$$

with $\lambda = \frac{1}{4} N^2 \mu_0 A_g$. Here N is the number of windings of the coils, μ_0 is the permeability of vacuum, A_g is surface area of the poles of the magnetic coil, g_0 is the nominal gap distance between the coil and the rotor, x is the displacement of rotor and its center position, i_{bias} is the bias current through the coils and i the control current. Note that due to the particular configuration of the differential driving mode the resulting magnetic force becomes a linear function of control current when the rotor is at its nominal position (i.e. $x=0$). Since the rotor will generally be operating closely around this nominal position, it makes sense to approximate equation (4) with a linear model. A first

order Taylor expansion around $i=0$ and $x=0$ yields

$$\mathbf{F}^{amb} = k_x x + k_i i \quad (5)$$

with $k_x = 4\lambda i_0^2 / g_0^3$ and $k_i = 4\lambda i_0 / g_0^2$.

Since k_x is always positive, (5) shows that an AMB has a negative stiffness. Since x describes the position of an unconstrained body, an unstable system is obtained. Therefore a stabilizing controller is needed to keep the spindle at the prescribed location.

4.4 Combining the models

A model of a milling spindle in magnetic bearings can be obtained as follows. In equation (2), the vector of generalized external forces \mathbf{F}_{ext} has the same dimension as the number of generalized coordinates. However, only at the location of the bearings and at the tooltip this vector will have nonzero components. Let us number the elements of the FE model, starting from the rear end of the spindle and ending at the tool tip. We will assume that the forces exerted by the rear and front magnetic bearing are concentrated at the 2nd node of element number N_A and N_B respectively (see figure 3b). The cutting force F_c is acting at the 2nd node of element number N . Combining the variables and parameters in vectors

$$\begin{aligned} \mathbf{F}^{amb} &= \begin{bmatrix} F_{x,A}^{amb} & F_{y,A}^{amb} & F_{x,B}^{amb} & F_{y,B}^{amb} \end{bmatrix}^T \\ \mathbf{F}_c &= \begin{bmatrix} F_{c,x} & F_{c,y} \end{bmatrix}^T, \mathbf{i} = \begin{bmatrix} i_{x,A} & i_{y,A} & i_{x,B} & i_{y,B} \end{bmatrix}^T \\ \mathbf{K}_x &= \text{diag}(k_x^{A,x}, k_x^{A,y}, k_x^{B,x}, k_x^{B,y}) \\ \mathbf{K}_i &= \text{diag}(k_i^{A,x}, k_i^{A,y}, k_i^{B,x}, k_i^{B,y}) \end{aligned}$$

we can write

$$\mathbf{F}_{ext} = \mathbf{B}^{amb} \mathbf{F}^{amb} + \mathbf{L} \mathbf{F}_c \quad (6)$$

where $\mathbf{B}^{amb} \in \mathfrak{R}^{4(N+1) \times 4}$, $\mathbf{L} \in \mathfrak{R}^{4(N+1) \times 2}$, and

$$B_{i,j} = \begin{cases} 1 & \text{for } \begin{matrix} i=4N_A+1, j=1 \\ i=4N_A+2, j=2 \\ i=4N_B+1, j=3 \\ i=4N_B+2, j=4 \end{matrix} \\ 0 & \text{otherwise} \end{cases}, \quad L_{i,j} = \begin{cases} 1 & \text{for } \begin{matrix} i=4N+1, j=1 \\ i=4N+2, j=2 \end{matrix} \\ 0 & \text{otherwise} \end{cases}$$

When we denote the positions of the rotor in x and y direction at the location of the bearings sensors with vector \mathbf{x}^{amb} , we may write

$$\mathbf{x}^{amb} = (\mathbf{B}^{amb})^T \mathbf{x} \quad (7)$$

$$\mathbf{F}^{amb} = \mathbf{K}_x \mathbf{x}^{amb} + \mathbf{K}_i \mathbf{i} \quad (8)$$

Combining (2), (6), (7) and (8), it follows that

$$\begin{aligned} \mathbf{M} \ddot{\mathbf{x}} + \mathbf{G} \dot{\mathbf{x}} + \left(\mathbf{K} - \mathbf{B}^{amb} \mathbf{K}_x (\mathbf{B}^{amb})^T \right) \mathbf{x} = \\ \mathbf{B}^{amb} \mathbf{K}_i \mathbf{i} + \mathbf{L} \mathbf{F}_c \end{aligned} \quad (9)$$

With vector \mathbf{y} representing the positions of the rotor in x and y direction at the location of the displacement sensors, we can derive a state space model for our spindle system:

$$\begin{aligned} \dot{\tilde{\mathbf{x}}} &= \mathbf{A} \tilde{\mathbf{x}} + \mathbf{B}_1 \mathbf{i} + \mathbf{B}_2 \mathbf{F}_c \\ \mathbf{y} &= \mathbf{C} \tilde{\mathbf{x}} \end{aligned} \quad (10)$$

Here $\tilde{\mathbf{x}} = [\mathbf{x} \quad \dot{\mathbf{x}}]$, and

$$\begin{aligned} \mathbf{A} &= \begin{bmatrix} \mathbf{0} & \mathbf{I} \\ -\mathbf{M}^{-1} \left(\mathbf{K} - \mathbf{B}^{amb} \mathbf{K}_x (\mathbf{B}^{amb})^T \right) & -\mathbf{M}^{-1} \mathbf{G} \end{bmatrix} \\ \mathbf{B}_1 &= \begin{bmatrix} \mathbf{0} \\ \mathbf{M}^{-1} \mathbf{B}^{amb} \mathbf{K}_i \end{bmatrix}, \mathbf{B}_2 = \begin{bmatrix} \mathbf{0} \\ \mathbf{M}^{-1} \mathbf{L} \end{bmatrix}, \mathbf{C} = \begin{bmatrix} \mathbf{C}^{amb} & \mathbf{0} \end{bmatrix} \end{aligned}$$

where $\mathbf{C}^{amb} \in \mathfrak{R}^{4 \times 4(N+1)}$ is constructed similarly as \mathbf{B}^{amb} . We can use this state space model for multiple purposes:

1. It provides us with a model of the transfer function of the cutting force on the tooltip to the displacements at the bearings.
2. By calculating the eigenvalues of the \mathbf{A} matrix, we can obtain the structural modal frequencies of the spindle. Matrix \mathbf{G} being dependent on the rotational speed, these frequencies will change on increasing rotational speed. This can be observed in figure 4 in which we have included a Campbell plot. This plot shows the modal frequencies as a function of the rotational speed for the spindle of our setup (with no tool attached).
3. It can be used in a model based estimation setup to estimate the unknown cutting force from measurements of \mathbf{y} and \mathbf{i} . This we will show in the next section.

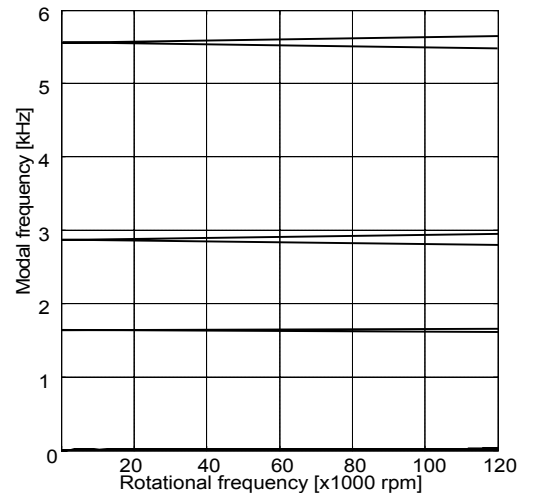


Figure 4: Campbell plot of AMB spindle.

5 CUTTING FORCE ESTIMATION

5.1 Problem definition

We consider magnetic bearing spindle system in its closed loop as depicted in figure 5. Transfer function \mathbf{H}_{amb} represents the magnetic bearing spindle system for which we developed a model in the previous section. The measurements of the displacements $\bar{\mathbf{y}}$ of the rotor are corrupted with measurement noise \mathbf{v}_1 , which is assumed to be additive. The controller \mathbf{H}_C takes these measurements as input and computes a signal for the current amplifier \mathbf{H}_A . The exact transfer function of the controller and the current amplifier are unknown. However, measurements of the currents through the AMB coils $\bar{\mathbf{i}}$ are available. The measurement noise \mathbf{v}_2 in these measurements is also assumed to be additive. With noisy measurements $\bar{\mathbf{y}}$ and $\bar{\mathbf{i}}$ available, the objective is to estimate the unknown cutting force \mathbf{F}_c .

5.2 Achievable bandwidth with indirect force estimation using AMBs

The first question that rises is to what extent the signals $\bar{\mathbf{y}}$ and $\bar{\mathbf{i}}$ contain information about the cutting force. To evaluate this, observe from figure 5 that we can write the measurements as filtered versions of the cutting force signal:

$$\begin{pmatrix} \bar{\mathbf{y}} \\ \bar{\mathbf{i}} \end{pmatrix} = \begin{bmatrix} \mathbf{S}\mathbf{H}_{amb,2} \\ -\mathbf{H}_A\mathbf{H}_C\mathbf{S}\mathbf{H}_{amb,2} \end{bmatrix} \mathbf{F}_c + \begin{bmatrix} \mathbf{S} \\ -\mathbf{H}_A\mathbf{H}_C\mathbf{S} \end{bmatrix} \begin{pmatrix} \mathbf{v}_1 \\ \mathbf{v}_2 \end{pmatrix} \quad (11)$$

with $\mathbf{S} = (\mathbf{I} + \mathbf{H}_{amb,1}\mathbf{H}_A\mathbf{H}_C)^{-1}$ and $\mathbf{H}_{amb,i}$ with $i=1,2$ the transfer function of the AMB spindle from the current and the cutting force respectively to the displacements at the sensor positions. The unknown $\mathbf{H}_A\mathbf{H}_C$ can be eliminated from this expression by constructing $\bar{\mathbf{z}} = \bar{\mathbf{y}} - \mathbf{H}_{amb,1}\bar{\mathbf{i}}$. It can be verified that

$$\bar{\mathbf{y}} - \mathbf{H}_{amb,1}\bar{\mathbf{i}} = \mathbf{H}_{amb,2}\mathbf{F}_c - \mathbf{H}_{amb,1}\mathbf{v}_2 + \mathbf{v}_1 \quad (12)$$

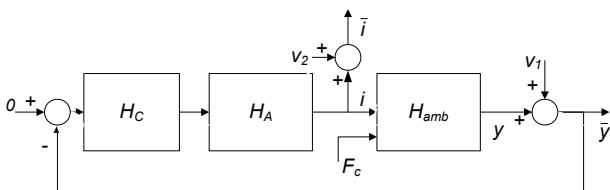


Figure 6: Measurement model of AMB spindle in closed loop.

which is equivalent to the system

$$\begin{aligned} \tilde{\mathbf{x}} &= \mathbf{A}\tilde{\mathbf{x}} + \mathbf{B}_1\bar{\mathbf{i}} + \mathbf{B}_2\mathbf{F}_c - \mathbf{B}_1\mathbf{v}_2 \\ \bar{\mathbf{y}} &= \mathbf{C}\tilde{\mathbf{x}} + \mathbf{v}_1 \end{aligned} \quad (13)$$

This shows that for solving the estimation problem, we can consider an open loop model of the AMB spindle. However, as the transfer function from \mathbf{v}_2 to $\bar{\mathbf{y}}$ in this model is unstable, we need to ensure that we will construct a stable estimator. In the next section we will return to this issue.

Derivational details omitting, it can be shown that the signal to noise ratio in $\bar{\mathbf{z}}$ is given by

$$SNR(\omega) = \frac{\text{tr}(F(\omega)\mathbf{H}_{amb,2}^H(j\omega)\mathbf{H}_{amb,2}(j\omega))}{4\bar{\sigma}_1^2 + \bar{\sigma}_2^2 \sum_i \mathbf{v}_i^2(\mathbf{H}_{amb,1}(j\omega))} \quad (14)$$

Here $\sum_i \mathbf{v}_i^2(\mathbf{H}_{amb,1}(j\omega))$ means the sum of all squared singular values of transfer function $\mathbf{H}_{amb,1}(j\omega)$, tr refers to the trace operator and the matrix superscript H refers to the complex conjugate transpose. $F(\omega)$ is the generalized power spectral density of the cutting forces. In the analysis, we have assumed that the noise on all measurements is uncorrelated and that all displacement and current measurements have equal variance $\bar{\sigma}_1^2$ and $\bar{\sigma}_2^2$ respectively. To evaluate $SNR(\omega)$ we can do the following. We assume a cutting force of a specific amplitude and frequency, as well as values for $\bar{\sigma}_1^2$ and $\bar{\sigma}_2^2$. The above equation provides the signal to noise ratio for that particular frequency. Evaluating this for the whole frequency range enables us to make a plot of the $SNR(\omega)$. In figure 6 we have done this for our setup, where based on sensor resolution we have taken $\bar{\sigma}_1 = 10^{-7}$ m and $\bar{\sigma}_2 = 10^{-3}$ A. A

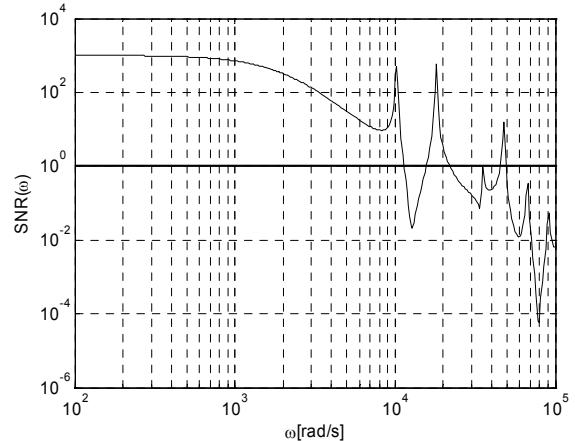


Figure 5: Signal to noise ratio plot.

cutting force with amplitude of $5N$ is assumed. For those frequencies where the SNR will be less than 1, the noise power in \mathbf{z} will exceed the power of the filtered cutting force in \mathbf{z} , making estimation of the cutting force from \mathbf{z} increasingly difficult. Hence the frequency where $SNR(\omega)$ becomes smaller than 1 is a good measure for the maximum achievable bandwidth that can be obtained. For our setup this is 11.7 krad/s (1.9 kHz) which corresponds to a rotational speed of 111 krpm. This shows that potentially a force signal can be obtained with sufficient bandwidth. As a comparison, cut-off frequencies of high-end force measurement setups of leading manufacturers are around 2 kHz.

5.3 Indirect force estimation by Augmented Kalman filtering

An approach that has been proposed by a few other authors to solve similar indirect force measurement problems, is to apply the Augmented Kalman filter structure (see e.g.[5,6]). The Kalman filter is an optimal linear state estimator. In the Augmented Kalman filter structure the unknown cutting force is modeled as a slowly varying state of the system which is driven by a white noise process with a specific variance. This effectively means that the unknown cutting force is modeled as a realization of a random walk process:

$$\dot{\mathbf{F}}_c = \mathbf{w} \quad (15)$$

with \mathbf{w} a white noise process with diagonal covariance matrix $\sigma_w^2 \mathbf{I}$. This type of modeling includes very limited a priori knowledge of the cutting forces and we will discuss the limitations of such modeling for force estimation in what follows. Here we will demonstrate that the approach can also be used in the case of indirect force measurement with AMB spindles. Combining our spindle model, cutting force model and measurement model, we can write:

$$\begin{bmatrix} \dot{\mathbf{x}} \\ \dot{\mathbf{F}}_c \end{bmatrix} = \begin{bmatrix} \mathbf{A} & \mathbf{B}_2 \\ \mathbf{0} & \mathbf{0} \end{bmatrix} \begin{bmatrix} \mathbf{x} \\ \mathbf{F}_c \end{bmatrix} + \begin{bmatrix} \mathbf{B}_1 \\ \mathbf{0} \end{bmatrix} \bar{\mathbf{i}} + \begin{bmatrix} -\mathbf{B}_1 & \mathbf{0} \\ \mathbf{0} & \mathbf{I} \end{bmatrix} \begin{bmatrix} \mathbf{v}_1 \\ \mathbf{w} \end{bmatrix}$$

$$\bar{\mathbf{y}} = \begin{bmatrix} \mathbf{C} & \mathbf{0} \end{bmatrix} \begin{bmatrix} \mathbf{x} \\ \mathbf{F}_c \end{bmatrix} + \mathbf{v}_2 \quad (16)$$

For this system a state estimator is designed with the following structure:

$$\begin{bmatrix} \dot{\hat{\mathbf{x}}} \\ \dot{\hat{\mathbf{F}}}_c \end{bmatrix} = \mathbf{A}_{aug} \begin{bmatrix} \hat{\mathbf{x}} \\ \hat{\mathbf{F}}_c \end{bmatrix} + \mathbf{B}_{aug} \bar{\mathbf{i}} + \mathbf{L} \left(\bar{\mathbf{y}} - \mathbf{C}_{aug} \begin{bmatrix} \hat{\mathbf{x}} \\ \hat{\mathbf{F}}_c \end{bmatrix} \right) \quad (17)$$

Here we have that

$$\mathbf{A}_{aug} = \begin{bmatrix} \mathbf{A} & \mathbf{B}_2 \\ \mathbf{0} & \mathbf{0} \end{bmatrix}, \quad \mathbf{B}_{aug} = \begin{bmatrix} \mathbf{B}_1 \\ \mathbf{0} \end{bmatrix}, \quad \mathbf{C}_{aug} = \begin{bmatrix} \mathbf{C} \\ \mathbf{0} \end{bmatrix},$$

while $\mathbf{L} = \mathbf{P} \mathbf{C}_{aug}^T \mathbf{R}^{-1}$, $\mathbf{R} = \sigma_w^2 \mathbf{I}$, and \mathbf{P} is the symmetric positive solution of the algebraic Ricatti equation

$$\mathbf{A}_{aug} \mathbf{P} + \mathbf{P} \mathbf{A}_{aug}^T + \mathbf{Q} + \mathbf{P} \mathbf{C}_{aug}^T \mathbf{R}^{-1} \mathbf{C}_{aug} \mathbf{P} = \mathbf{0} \quad (18)$$

with $\mathbf{Q} = \text{diag}(\sigma_{v_1}^2 \mathbf{B}_1 \mathbf{B}_1^T, \sigma_w \mathbf{I})$. A well known result from linear estimation theory states that the above filter will be asymptotically stable if and only if system (16) is detectable, i.e. if $\begin{bmatrix} \lambda \mathbf{I} - \mathbf{A}_{aug}^T & \mathbf{C}_{aug}^T \end{bmatrix}$ has constant rank for all λ

with $\text{Re}(\lambda) > 0$. Without going into full detail, it can be verified for the presented force estimator that this condition is indeed satisfied. One of requirements for this to be the case is that (\mathbf{C}, \mathbf{A}) is detectable. Detectability of (\mathbf{C}, \mathbf{A}) follows from the structure of our AMB system. Loosely we could state that this condition implies that all unstable modes of the rotor can be observed through the sensors.

Equation (17) indeed shows that the estimator takes the current and displacement measurements as inputs, and calculates an estimate of the cutting forces (as well as for the state of our system).

6 SIMULATION RESULTS

The described model and estimator have been implemented in Matlab/Simulink. The number of elements that have been used for the spindle is 63, and for the tool 30. This results in a model with 752 states. The response of this system to a cutting force is simulated, where we have taken a cutting force signal that is constructed according to a model described by Dow [7]. The rotational frequency is 10,000 rpm. Figure 7 shows a plot of the simulated displacement sensor reading and the current sensor reading of the front radial x bearing.

To obtain an estimator, first balanced truncation is applied to reduce the model order to 20 states [8]. This results in a model that includes the first three flexible modes, the highest having an eigenfrequency of around 35 krad/s. As can be observed from the SNR plot of figure 6, this suffices for constructing an estimator. A good estimator is obtained by choosing $\sigma_w = 1 \cdot 10^5$. Here an engineering approach is chosen. If the value is decreased, this implies we model our cutting force signal as a more slowly varying signal, resulting in more smooth

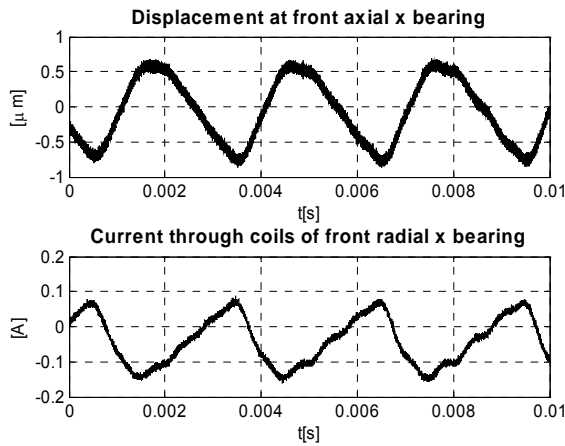


Figure 7: Simulation of AMB spindle.

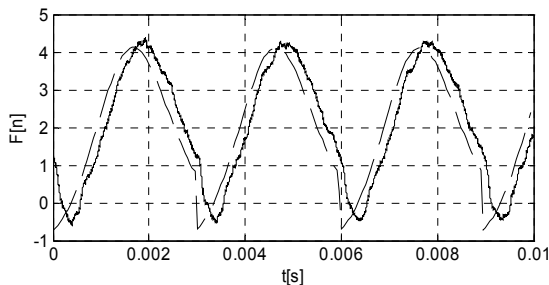


Figure 8: Real (dashed) and estimated (solid) cutting force in x-direction.

estimates with consequently less detail. On the other hand, increasing the σ_w will increase the details in the force estimates, while more of such details will in fact be noise. This shows the limitation of modeling the cutting force as a random walk process.

The force estimation result of the Augmented Kalman filter for the x-direction is pictured in figure 8. Although a phase delay can be observed, the force estimates are in good correspondence with the actual forces.

7 CONCLUSIONS

We have demonstrated that indirect measurement of the cutting forces in a micromilling application can be achieved by using the active nature of an Active Magnetic Bearing (AMB) spindle. For this appropriate modeling of the spindle and AMB dynamics as well as the cutting forces is needed to obtain reliable results. The bandwidth that can be realized with this approach is high enough for the micromilling application.

8 OUTLOOK

Future research will include more generic estimation approaches, including extended modeling of the cutting force signal. Experimental validation will be performed to demonstrate the methodology in practice. Furthermore we intend to develop monitoring and control tech-

niques based on the obtained force signal, such as tool deflection compensation and force controlled milling. For these also the active nature of the AMB can be used.

9 ACKNOWLEDGEMENTS

Part of this research was funded by MicroNed and the Delft Center of Mechatronics and Microsystems.

10 REFERENCES

- [1] Bleuler, H., Gähler, C., Herzog, R., Larssonneur, R., Mizuno, T., Siegwart, R., Woo, S.J., Application of Digital Signal Processors for Industrial Magnetic Bearings, IEEE Transactions on Control Systems Technology, Vol 2., No. 4, December 1994, 280-289
- [2] Müller, M.K., On-Line Process Monitoring in High Speed Milling with an Active Magnetic Bearing Spindle, Dissertation, ETH Zürich, 2002.
- [3] Auchet, S., Chevrier, P., Lacour, M., Lipinski, P., A new method of cutting force measurement based on command voltages of active electro-magnetic bearings, Int J of Mach Tools & Manuf 44 (2004) 1441-1449
- [4] Schweitzer, G., Bleuler, H., Traxler, A., Active Magnetic Bearings, Hochschulverlag AG, ETH Zürich, 1994.
- [5] Altintas, Y., Park, S.S., Dynamic compensation of Spindle-Integrated Force Sensors, Annals of the CIRP, 53/1:305-308S.S.
- [6] Park, S.S, Altintas, Y., Dynamic Compensation of Spindle Integrated Force Sensors with Kalman Filter, Journal of Dynamic Systems, Measurement and Control, Transactions of the ASME, Vol. 126, September 2004, 443-452.
- [7] Dow, T.A., Miller, E.L., Garrard, K., Tool force and deflection compensation for small milling tools, Precision Engineering 28 (2004) 31-45.
- [8] Obinata, G., Anderson, B.D.O., Model reduction for control system design, Springer, London, 2001